Nanoscale

Accepted Manuscript

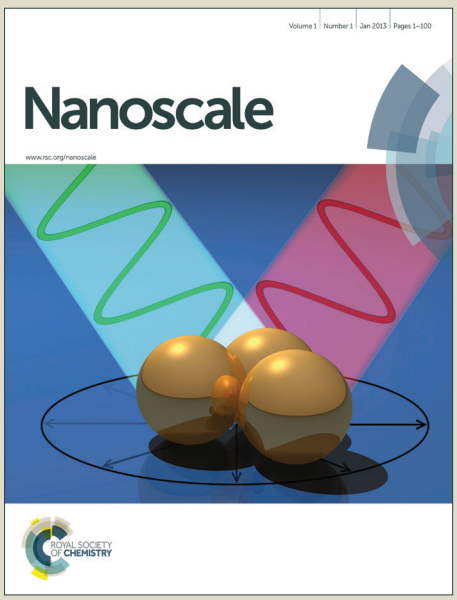

ROYAL SOCIETY OF CHEMISTRY

www.rsc.org/nanoscale

Cite this: DOI: 10.1039/c0xx00000x

www.rsc.org/xxxxxx

ARTICLE TYPE

A promising monolayer membrane for oxygen separation from harmful gases: Nitrogen-substituted polyphenylene

Ruifeng Lu,*[a] Zhaoshun Meng,[a] Dewei Rao,[b] Yunhui Wang,[a] Qi Shi,[a] Yadong Zhang,[a] Erjun Kan,[a,c] Chuanyun Xiao*[a,c] and Kaiming Deng*[a,c]

Received (in XXX, XXX) Xth XXXXXXXXX 20XX, Accepted Xth XXXXXXXXX 20XX
DOI: 10.1039/b000000x

We theoretically demonstrate that N substitutional doping dramatically reduces the diffusion barrier of oxygen passing through the pores of polyphenlene, leading to a colossal enhancement in O_2 selectivity over various harmful gases with an excellent permeance at appropriate temperatures for O_2 across one N doped polyphenylene in unit cell.

Since graphene was fabricated in experiment,[1] much attention has been paid to two-dimensional materials for their extensive potential applications. Despite graphene has a series of tempting properties and can be used in a wide range of areas, its performance for gas permeation is not good even for noble gas helium, as demonstrated both experimentally[2] and theoretically.[3] In order to increase the gas permeability through graphene, drilling holes via either electron beam punching[4] or chemical etching after covering a layer of substrate[5] on the perfect graphene have been employed as common techniques. By rationally designing the adjustable pores on graphene, pioneering theoretical investigations for selective ion passage,[6] gas[7] and isotope separation[8] have been carried out. In these works, nitrogen substitution is found to be an appropriate way to fine tune the pore shape and size for optimal separation properties.

Excitingly, a porous graphene (PG) with periodic pores, known as "polyphenylene", has been synthesized by surface-assisted coupling of specifically designed molecular building blocks.[9] The ideal membrane should be thin enough and have pores as uniform as possible to guarantee desired permeance and selectivity. PG is an excellent candidate because of its one-atom thickness and well-defined pores, and it turns out to be a perfect atmospheric nanofilter in favor of H_2 and He.[10] As a single layer membrane, it can be used not only for isotopic He separation[11] but also for hydrogen purification from those with larger kinetic diameters including oxygen, carbon monoxide, carbon dioxide, and methane.[12] As suggested recently, monolayer graphene-based materials could be hopefully utilized for water desalination.[13] In this work, we will show that the multifunctional PG possesses undiscovered potential beyond the above mentioned applications.

Oxygen purification or separation is of great importance in many fields, such as medical treatment and industry. The gas mask, which requires good performance of rejecting harmful gases while not blocking oxygen, is a necessary under the situations of a fire accident or toxic gases leaking from chemical plants. As a result, oxygen separation from poisonous or pungent gases is worth studying for its valuable perspective. Although there have been many studies on oxygen permeation through the mixed ionic-electronic conducting ceramic-based membranes,[14] two-dimensional carbon materials as oxygen separation membranes have not been systematically studied to our knowledge. For this purpose, we explored the effect of nitrogen substitution in PG on the performance of oxygen separation from various harmful gases.

Nowadays, computational simulations play a more and more important role in developing various materials with desired properties. For example, based on our first-principles investigation[15] of Li-doped conjugated microporous polymer as a potential hydrogen storage medium, we have succeeded in synthesized such a material, achieving a promising capacity for reversible hydrogen storage.[16] Most recently, K. Celebi *et al.*[17] reported that from prediction of two-dimensional transport theory, a physically perforated double-layer graphene shows highly efficient mass transfer and the measured transport rates are in agreement with theoretical values. These studies demonstrate that rational materials design from theory could lead to practical application in gas storage and separation.

As is well known, N doping of carbon nanotubes and graphene can be readily accomplished in laboratory,[18] and N-doped carbon materials have versatile applications in supercapacitor,[19] lithium battery,[20] catalysis,[21] biosensing,[22] nanoelectronics,[23] etc. To realize N-substituted PG, the possible route is to assemble the building blocks, N-contained cyclohexa-*m*-phenylene synthesized by Suzuki reactions,[24] from the surface-promoted coupling on metal surface,[9,25] or to dope N in PG through electrothermal reactions with ammonia.[26]

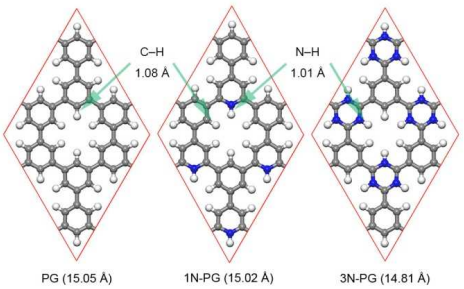

Fig. 1 The structures of PG, 1N-PG, and 3N-PG as well as their lattice parameters (in the parentheses) of 2×2×1 supercells. (C, gray balls; H, white balls; N, blue balls).

Cite this: DOI: 10.1039/c0xx00000x

www.rsc.org/xxxxxx

ARTICLE TYPE

Table 1 Adsorption energies (E_{ad}, in eV)[a] of the studied gases on PG-based membranes, diffusion barriers ($E_{barrier}$, in eV)[b] of gases and selectivities (S, at T = 300 K)[c] of O_2 over harmful gases (X) when penetrating through the pores.

Membrane	Property	O_2	CO	Cl_2	HCN	NO	CO_2	SO_2	H_2S	HF
PG	E_{ad}	0.18	0.24	0.13	0.35	0.22	0.20	0.24	0.14	0.24
	$E_{barrier}$	1.12	2.28	2.43	2.21	1.84	1.93	3.71	4.15	0.81
	$S_{(O_2/X)}$	–	3×10^{19}	1×10^{22}	2×10^{18}	1×10^{12}	4×10^{13}	3×10^{43}	6×10^{50}	6×10^{-6}
1N-PG	E_{ad}	0.61	0.29	0.33	0.39	0.53	0.23	0.50	0.12	0.28
	$E_{barrier}$	0.05	2.18	1.75	2.11	1.06	2.14	3.33	4.13	0.85
	$S_{(O_2/X)}$	–	5×10^{35}	3×10^{28}	4×10^{34}	1×10^{17}	1×10^{35}	9×10^{54}	3×10^{68}	3×10^{13}
3N-PG	E_{ad}	1.27	0.41	0.37	0.49	0.81	0.28	0.63	0.47	0.34
	$E_{barrier}$	0.01	1.84	1.46	1.69	0.64	2.31	3.04	3.54	0.80
	$S_{(O_2/X)}$	–	6×10^{30}	2×10^{24}	2×10^{28}	4×10^{10}	5×10^{38}	6×10^{50}	2×10^{59}	2×10^{13}

[a] $E_{ad}= E_x + E_m - E_{x@m}$, where $E_{x@m}$, E_x and E_m are the total energies per supercell of optimized structures for gas adsorbed on PG-based membranes, isolated gas molecules and monolayer membranes, respectively. [b] $E_{barrier}=E_{TS}-E_r$, where E_{TS} and E_r represent the energies of the optimized transition state and reactant, respectively. [c] $S=A_{oxygen}/A_X$, where A_{oxygen} and A_X respectively stand for the diffusion rates of oxygen and other gases, please refer to the details in the main text.

Fig. 1 displays the structures of PG, one N doped in unit cell of PG (1N-PG) and three N doped in unit cell of PG (3N-PG). The lattice parameters of these three structures are only slightly different. After N substitution, the bond lengths with H are shortened from 1.08 Å of CH to 1.01 Å of NH, and the pore shape transforms a little bit. Nevertheless, the van der Waals pore sizes determined by the inscribed spheres within the pore are still smaller than the kinetic parameter (3.5 Å) of O_2.[27] In typical size sieving, the key factor is the pore width of membranes with respect to the kinetic diameters of the target molecular gases, which is only able to explain the classical transmission of gas with kinetic diameters obviously different from other gases and comparable to the pore width.[28]

Table 1 presents the diffusion barriers of various gases passing through the pores of PG, 1N-PG and 3N-PG. The corresponding optimized structures and their total energies can be found in the ESI†. The diffusion barrier for O_2 across PG is 1.12 eV, close to 1.13 eV calculated by Blankenburg *et al.*.[10] The barriers for CO and CO_2 across PG are almost the same as the reported values.[12] These agreements ensure our methods and results reliable. Remarkably, 1N-PG has a diffusion barrier of only 0.05 eV for O_2, which is even lower than those for H_2 across PG (0.37 eV)[10] and graphdiyne (0.10 eV).[29] From Table 1, it is easy to summarize that N substitution dramatically reduces the energy barrier for O_2 penetration through PG, which tells us that the kinetic diameter cannot be used to predict the diffusion property for our membrane.

Why does N substitution significantly reduce the diffusion barrier in 1N-PG and 3N-PG? The electron density isosurfaces of the transition state (TS) structures for O_2 passing through the pores in Fig. 2 help us to answer this question. Clearly, O_2 has the "most" electron overlaps with adjacent atoms of six orientations in PG, which compares with five orientations in 1N-PG and three in 3N-PG. Accordingly, the diffusion barrier of O_2 across PG is the highest while that of O_2 across 3N-PG is the lowest. This phenomenon can be observed for other gases (CO, Cl_2, HCN, NO, see in Fig. S1-S4†) and can be elucidated by the fact that N has a larger electronegativity than C accompanying the bond length with H shortened and the electron density more localized. Therefore, the overlapped electron densities at the pores act to repel the gas molecules to diffuse through the pores, which is consistent with the finding in previous work.[12] However, that obvious difference in the electron density can not be easily illustrated for the nonlinear molecules (SO_2, H_2S; see Fig. S6, Fig. S7†) because the magnitude of the overlapping can not be quantitatively determined, and the simple explanation doesn't work for CO_2 (Fig. S5†) whose diffusion barrier increases contrarily when N is doped in PG. Therefore, we further perform Mulliken charge analysis for the TS geometries. One can see in Figs. S8-S15† that the electroneutrality of PG is changed by N doping. It induces a more than triple increased net positive charge on the adjacent C atoms of N. The charge populations of the TS structures clearly indicate that the repulsive interaction will be enhanced between the positively charged C atom (located on the pore center) of CO_2 and C atoms of N-doped PG (neighboring to N) with significantly increased positive charge. For comparison, the S atom of SO_2 and H_2S and the O atom of O_2 of the TS geometries are negatively charged, leading to a lower barrier from attractive interactions with positively charged C atoms close to N. This should be the reason why the barrier of CO_2 changes with increasing of N very differently from O_2, SO_2, H_2S, etc. Our population analyses are consistent with the finding in the study of CO and O_2 adsorptions in vertically aligned N-doped carbon nanotubes.[18a] Thus, N-substituted PG can be regarded as a chemical affinity sieving[28] where the N doping modifies the chemical environments at the rims of the pores. Moreover, N doping has little influence on the diffusion barrier of HF, which has the lowest $E_{barrier}$ across PG.

Table 1 also lists the adsorption energies for the most stable configurations of gas molecules on top of the pores, which are all

larger than that of H_2 adsorbed on PG (0.03 eV),[10] indicating stronger van der Waals interactions. The introduction of N lone pairs enhances the adsorption of almost all the studied gases on the porous sheets. In particular, the adsorption energy of O_2 on 1N-PG is 0.61 eV, which implies a relatively stable binding between O_2 and 1N-PG, however, the absolute value of this energy is still smaller than the diffusion barrier of 0.85 eV for HF across 1N-PG, so desorption can be conducted at appropriate temperatures. Although the 3N-PG membrane has a lower O_2 energy barrier than 1N-PG, it is not useful for practical applications. On one hand, the higher the doping concentration is, the larger the formation energy per atom will be, in other words, the more difficult the doping becomes.[30] On the other hand, the large adsorption energy (1.27 eV) of O_2 on 3N-PG means that O_2 will be trapped near the pore, and it is difficult to diffuse far away. Therefore, in the following, we will focus on discussing the properties of the PG and the 1N-PG membranes in terms of N substitution effect on O_2 separation. The N substitution also lowers the diffusion barriers of some harmful gases; however, it is much more difficult for these harmful gases to diffuse through the pores than O_2 at ambient temperature when simply compare their barriers.

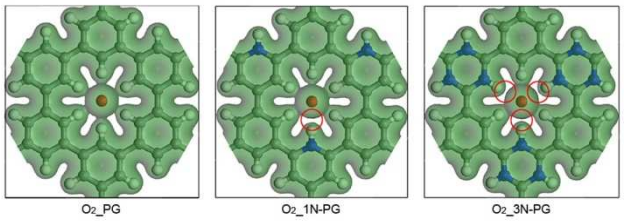

Fig. 2 Electron densities of the transition-state structures for O_2 passing through PG, 1N-PG and 3N-PG. The isovalue is 0.15 a.u. (C, gray balls; H, white balls; N, blue balls; O, red balls).

To quantitatively understand the performance of the proposed membrane, we calculated the selectivity and the permeance of the PG-based membrane. With regard to the selectivity for separating O_2 from the harmful gases, the Arrhenius equation is adopted: $A = A_0\exp(-E_{barrier}/k_BT)$, in which A is the diffusion rate, A_0 is the diffusion prefactor, $E_{barrier}$ is the diffusion barrier, k_B is the Boltzmann constant, and T is the temperature. Here we assume that the diffusion prefactors are identical for all gases under study.[12] Since the value turns out to be of the order of 10^{11} s^{-1} for all gases,[10] this assumption is reasonable to make meaningful conclusions. So we get the selectivity as: $S=A_{oxygen}/A_X=\exp(-(E_{oxygen}-E_X)/k_BT)$, where A_{oxygen} (E_{oxygen}) and A_X (E_X) respectively stand for the diffusion rates (diffusion barriers) of oxygen and other gases. In Fig. 3, the selectivities of O_2 over the selected poisonous and pungent gases across the PG and the 1N-PG membranes are plotted. The selectivity of O_2 over HF is not included in this figure, because HF has a lower diffusion barrier than O_2 in PG and the situation is reversed after N substitution, which already indicates a better performance of 1N-PG than PG. We can see from the figure that 1N-PG outperforms PG for the separation of O_2 from all the harmful gases in the whole temperature range. The selectivities of O_2 over the harmful gases at the room temperature of 300 K are also listed in Table 1. It is obvious that 1N-PG performs perfectly with the selectivity enhancement by 10^5 to 10^{22} times.

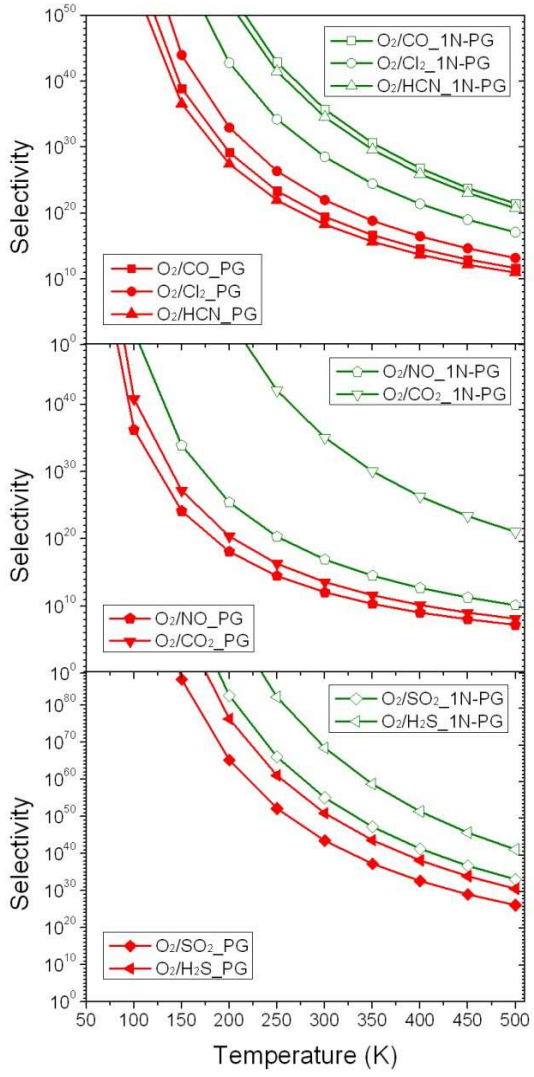

Fig. 3 Selectivities of O_2 over CO, Cl_2, HCN (top panel), NO and CO_2 (middle panel), SO_2 and H_2S (bottom panel) when penetrating through PG and 1N-PG.

The performance of a membrane is characterized not only by its selectivity but also by its permeance. The permeance is computed by $P = F/\Delta p$, where F is the molar flux (mol m^{-2} s^{-1}) of the gases, and Δp is the pressure difference (Pa) across the membrane. The molar flux F is determined by $F = N\times f$, in which N and f represent, respectively, the number of gas particles colliding with the wall and the probability for a particle to diffuse through the pore at a given velocity. Derived from the kinetic theory of gases, $N = p/(A\times(2\pi m k_BT)^{1/2})$, with p, A, m, k_B, and T denoting the pressure, Avogadro constant, the mass of the molecule, Boltzmann constant, and the temperature, respectively.[31] The probability f is given by $f = \int_{v_B}^{\infty} f(v)dv$, where $f(v)$ is the Maxwell velocity distribution and v_B represents the velocity corresponding to the diffusion barrier[10] (except for O_2, the higher adsorption energy of 0.61 eV instead of the diffusion barrier is taken to consider desorption of oxygen from the membrane). We set the incoming pressure p to be 3×10^5 Pa and the pressure difference Δp to be 10^5 Pa,[32] and the calculated

permeances of the studied gases are provided in Fig. 4. Except for CO_2 and HF, which have larger diffusion barriers in 1N-PG (Table 1), other harmful gases show limited increments in their permeances after N substitution, which corresponds to the decrease in their diffusion barriers. Fortunately, all the curves in Figure 4 of the harmful gases lie underneath the dashed line up to 500 K, which stands for the industrially acceptable permeance for gas separation.[33] For O_2, 1N-PG indicates an excellent behavior for its high permeance above 400 K, exceeding the industrial standard by around 2 orders of magnitude at 500 K. The O_2 permeance of 3.3×10^{-7} mol m^{-2} s^{-1} Pa^{-1} at 500 K for 1N-PG (i.e., the O_2 molar flux of 3.3×10^{-6} mol cm^{-2} s^{-1} at 10^5 Pa), is larger than all reported values at higher temperatures (600~1000 K)[14b,14c] of the mixed ionic-electronic conducting ceramic-based membranes.

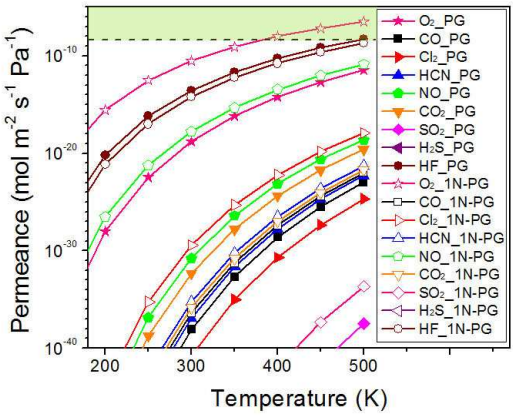

Fig. 4 Permeances versus temperature for the studied gases passing through PG and 1N-PG. Solid and hollow symbols correspond to the PG and 1N-PG membranes, respectively. Dashed line stands for the industrially acceptable permeance for gas separation.[22]

Conclusions

In summary, we have theoretically investigated the diffusion properties of O_2 and various harmful gases through the pristine PG and N-substituted PG. Due to the weakening in the overlapping of atomic electron density at the pores, the diffusion barrier of oxygen molecule decreases greatly after N substitution. Based on the first principles results, we have obtained very fascinating selectivities for the O_2 separation from the harmful gases as well as extremely high permeances for O_2 passing through one-N-doped PG at near ambient conditions. Please keep in mind that it is too difficult for other larger gas molecules not considered in this work, such as phosgene, alkane and alkene, etc., to penetrate the PG-based membrane. Therefore, in view of the successful controlled synthesis and doping technology, the N-doped PG as a very promising monolayer membrane for oxygen purification or oxygen separation from other gases, will be of great interest and utility in scientific research, industrial and medical areas, and also in daily life of human beings.

Computational methods

All the calculations were performed with the Dmol^3 module of Materials Studio 5.5 program[34] using the PBE exchange-correlation functional with the dispersion correlation of Grimme's scheme.[35] Periodic boundary conditions were applied, and the vacuum space of 18 Å is large enough to avoid the interaction of periodic images. During the geometric optimization, *z*-fixed layers in a 2×2×1 supercell were used and the convergence criteria were 1×10^{-5} Hartree in energy, 2×10^{-3} Hartree/Å in Hellmann-Feynman force, and 5×10^{-3} Å in atomic displacement. The criterion of self-consistent field computation in energy was chosen to be 1×10^{-6} Hartree and the smearing of 5×10^{-4} Hartree in energy was set to accelerate the convergence. The Brillouin zone was sampled by 6×6×1 *k*-point grid. For the transition state calculations, we employed the algorithm of linear synchronous transit maximization, followed by repeated conjugated gradient (CG) minimizations, and then quadratic synchronous transit maximizations and repeated CG minimizations until a transition state is located.[36]

Acknowledgments

This work was supported by NSF of China Grant No. 11174150 and 21373113, the Fundamental Research Funds for the Central Universities (No. 30920140111008, 30920140132037), and the Special Foundation for Ph.D. Programs of the Ministry of Education of China with Grant No. 20113219110032.

Notes and references

[a] *Department of Applied Physics, Nanjing University of Science and Technology, Nanjing 210094, P.R. China. E-mail: rflu@njust.edu.cn*
[b] *Institute for Advanced Materials, Jiangsu University, Zhenjiang 212013, P.R. China*
[c] *Key Laboratory of Soft Chemistry and Functional Materials, Ministry of Education, Nanjing University of Science and Technology, Nanjing 210094, P.R. China. E-mail: cxiao@njust.edu.cn; kmdeng@njust.edu.cn*

† Electronic Supplementary Information (ESI) available: Electron densities and Mulliken charge analyses of the transition-state geometries, the initial, transition-state, final configurations, and their total energies for the studied gases passing through PG-based membranes. See DOI: 10.1039/b000000x/

1 (a) Y. B. Zhang, J. P. Small, W. V. Pontius and P. Kim, *Appl. Phys. Lett.,* 2005, **86**, 073104; (b) K. S. Novoselov, D. Jiang, F. Schedin, T. J. Booth, V. V. Khotkevich, S. V. Morozov and A. K. Geim, *Proc. Natl. Acad. Sci. USA,* 2005, **102**, 10451-10453; (c) A. K. Geim and K. S. Novoselov, *Nat. Mater.,* 2007, **6**, 183-191; (d) J. S. Bunch, A. M. van der Zande, S. S. Verbridge, I. W. Frank, D. M. Tanenbaum, J. M. Parpia, H. G. Craighead and P. L. McEuen, *Science,* 2007, **315**, 490-493; (e) J. C. Meyer, A. K. Geim, M. I. Katsnelson, K. S. Novoselov, T. J. Booth and S. Roth, *Nature,* 2007, **446**, 60-63.
2 J. S. Bunch, S. S. Verbridge, J. S. Alden, A. M. van der Zande, J. M. Parpia, H. G. Craighead and P. L. McEuen, *Nano Lett.,* 2008, **8**, 2458-2462.
3 O. Leenaerts, B. Partoens and F. M. Peeters, *Appl. Phys. Lett.,* 2008, **93**, 193107.
4 M. D. Fischbein and M. Drndić, *Appl. Phys. Lett.,* 2008, **93**, 113107.
5 (a) A. J. Du and S. C. Smith, *J. Phys. Chem. Lett.,* 2011, **2**, 73-80; (b) S. P. Koenig, L. D. Wang, J. Pellegrino and J. S. Bunch, *Nat. Nanotech.,* 2012, **7**, 728-732.
6 K. Sint, B. Y. Wang and P. Král, *J. Am. Chem. Soc.,* 2008, **130**, 16448-16449.
7 (a) D. E. Jiang, V. R. Cooper and S. Dai, *Nano Lett.,* 2009, **9**, 4019-4024; (b) M. X. Shan, Q. Z. Xue, N. N. Jing, C. C. Ling, T. Zhang, Z. F. Yan and J. T. Zheng, *Nanoscale,* 2012, **4**, 5477-5482.
8 (a) M. Hankel, Y. Jiao, A. J. Du, S. K. Gray and S. C. Smith, *J. Phys. Chem. C,* 2012, **116**, 6672-6676; (b) A. W. Hauser and P. Schwerdtfeger, *J. Phys. Chem. Lett.,* 2012, **3**, 209-213.

9 M. Bieri, M. Treier, J. M. Cai, K. Aït-Mansour, P. Ruffieux, O. Gröning, P. Gröning, M. Kastler, R. Rieger, X. L. Feng, K. Müllen and R. Fasel, *Chem. Commun.,* 2009, **45**, 6919-6921.

10 S. Blankenburg, M. Bieri, R. Fasel, K. Müllen, C. A. Pignedoli and D. Passerone, *Small,* 2010, **6**, 2266-2271.

11 J. Schrier, *J. Phys. Chem. Lett.,* 2010, **1**, 2284-2287.

12 (a) Y. F. Li, Z. Zhou, P. W. Shen and Z. F. Chen, *Chem. Commun.,* 2010, **46**, 3672-3674; (b) Q. Tang, Z. Zhou and Z. F. Chen, *Nanoscale,* 2013, **5**, 4541-4583.

13 E. N. Wang and R. Karnik, *Nat. Nanotech.,* 2012, **7**, 552-554.

14 (a) H. H. Wang, S. Werth, T. Schiestel and J. Caro, *Angew. Chem. Int. Ed.,* 2005, **44**, 6906-6909; (b) J. Sunarso, S. Baumann, J. M. Serra, W. A. Meulenberg, S. Liu, Y. S. Lin and J. C. Diniz da Costa, *J. Membr. Sci.*, 2008, **320**, 13-41. (c) Y. Liu, X. F. Zhu, M. R. Li, H. Y. Liu, Y. Cong and W. S. Yang, *Angew. Chem. Int. Ed.,* 2013, **52**, 3232-3236.

15 R. F. Lu, A. Li and W. Q. Deng, *Commun. Comput. Chem.*, 2013, **1**, 27-39.

16 A. Li, R. F. Lu, Y. Wang, X. Wang, K. L. Han and W. Q. Deng, *Angew. Chem. Int. Ed.*, 2010, **49**, 3330-3333.

17 K. Celebi, J. Buchheim, R. M. Wyss, A. Droudian, P. Gasser, I. Shorubalko, J. I. Kye, C. Lee and H. G. Park, *Science*, 2014, **344**, 289-292.

18 (a) K. P. Gong, F. Du, Z. H. Xia, M. Durstock and L. M. Dai, *Science*, 2009, **323**, 760-764; (b) L. S. Panchakarla, K. S. Subrahmanyam, S. K. Saha, A. Govindaraj, H. R. Krishnamurthy, U. V. Waghmare and C. N. R. Rao, *Adv. Mater.*, 2009, **21**, 4726-4730; (c) H. B. Wang, T. Maiyalagan and X. Wang, *ACS Catal.*, 2012, **2**, 781-794; (d) K. N. Wood, R. O'Hayre and S. Pylypenko, *Energy Environ. Sci.*, 2014, **7**, 1212-1249.

19 (a) Z. H. Wen, X. C. Wang, S. Mao, Z. Bo, H. Kim, S. M. Cui, G. H. Lu, X. L. Feng and J. H. Chen, *Adv. Mater.*, 2012, **24**, 5610-5616; (b) B. You, L. L. Wang, L. Yao and J. Yang, *Chem. Commun.*, 2013, **49**, 5016-5018.

20 (a) A. L. M. Reddy, A. Srivastava, S. R. Gowda, H. Gullapalli, M. Dubey and P. M. Ajayan, *ACS Nano*, 2010, **4**, 6337-6342; (b) Z. S. Wu, W. C. Ren, L. Xu, F. Li and H. M. Cheng, *ACS Nano*, 2011, **5**, 5463-5471.

21 (a) M. K. Liu, Y. F. Song, S. X. He, W. W. Tjiu, J. S. Pan, Y. Y. Xia and T. X. Liu, *ACS Appl. Mater. Interfaces*, 2014, **6**, 4214-4222; (b) L. T. Qu, Y. Liu, J. B. Baek and L. M. Dai, *ACS Nano*, 2010, **4**, 1321-1326.

22 Y. Wang, Y. Y. Shao, D. W. Matson, J. H. Li and Y. H. Lin, *ACS Nano*, 2010, **4**, 1790-1798.

23 (a) D. C. Wei, Y. Q. Liu, Y. Wang, H. L. Zhang, L. P. Huang and G. Yu, *Nano Lett.*, 2009, **9**, 1752-1758; (b) D. Usachov, O. Vilkov, A. Grüneis, D. Haberer, A. Fedorov, V. K. Adamchuk, A. B. Preobrajenski, P. Dudin, A. Barinov, M. Oehzelt, C. Laubschat and D. V. Vyalikh, *Nano Lett.*, 2011, **11**, 5401-5407.

24 W. Pisula, M. Kastler, C. Yang, V. Enkelmann and K. Müllen, *Chem. Asian J.,* 2007, **2**, 51-56.

25 M. Bieri, M. T. Nguyen, O. Gröning, J. M. Cai, M. Treier, K. Aït-Mansour, P. Ruffieux, C. A. Pignedoli, D. Passerone, M. Kastler, K. Müllen and R. Fasel, *J. Am. Chem. Soc.,* 2010, **132**, 16669-16676.

26 X. R. Wang, X. L. Li, L. Zhang, Y. Yoon, P. K. Weber, H. L. Wang, J. Guo and H. J. Dai, *Science,* 2009, **324**, 768-771.

27 D. W. Brech, *Zeolites Molecular Sieves: Structure, Chemistry and Use*, Wiley, New York, 1973.

28 Y. Jiao, A. J. Du, M. Hankel and S. C. Smith, *Phys. Chem. Chem. Phys.,* 2013, **15**, 4832-4843.

29 Y. Jiao, A. J. Du, M. Hankel, Z. H. Zhu, V. Rudolph and S. C. Smith, *Chem. Commun.,* 2011, **47**, 11843-11845.

30 R. F. Lu, D. W. Rao, Z. L. Lu, J. C. Qian, F. Li, H. P. Wu, Y. Q. Wang, C. Y. Xiao, K. M. Deng, E. J. Kan and W. Q. Deng, *J. Phys. Chem. C,* 2012, **116**, 21291-21296.

31 A. W. Hauser, J. Schrier and P. Schwerdtfeger, *J. Phys. Chem. C,* 2012, **116**, 10819-10827.

32 S. T. Oyama, D. Lee, P. Hacarlioglu and R. F. Saraf, *J. Membr. Sci.,* 2004, **244**, 45-53.

33 Z. Q. Zhu, *J. Membr. Sci.,* 2006, **281**, 754-756.

34 (a) B. Delley, *J. Chem. Phys.*, 1990, **92**, 508−517; (b) B. Delley, *J. Chem. Phys.*, 2000, **113**, 7756−7764.

35 S. Grimme, *J. Comput. Chem.,* 2006, **27**, 1787-1799.

36 N. Govind, M. Petersen, G. Fitzgerald, D. King-Smith and J. Andzelm, *Comput. Mater. Sci.,* 2003, **28**, 250-258.